



SD-R1

**State-of-the Art Report  
SEISMIC OBSERVATIONS AND VIBRATION TESTS  
FOR VERIFICATION OF SSI ANALYSIS METHODS**

Hiroshi TAJIMI

Tajimi Engineering Services, LTD., Shinjuku-ku, Tokyo, Japan

SUMMARY

This paper describes the state-of-the-art report for the Sub-Theme 1 in the Special Theme Session SD, entitled by "Dynamic soil-structure interaction: verification and design application." The paper reviews a few but significant experimental data available up to the present time to validate the current SSI analysis methods, as derived from seismic observations and field shaker tests. Some suggestions are made for future development.

INTRODUCTION

Recently, a remarkable progress has been made in theoretically studying the soil-structure interaction (SSI) problems and in particular, in evaluating the dynamic characteristics of embedded structures. The practical application of the SSI analysis has been also developed to compute the seismic response of important structures such as nuclear power plants, bridge abutments, high-rise buildings on pile foundations, and so on. However, as the practical analysis aims to predict overall response of a large system composed of soil and structure during an earthquake, it necessarily involves a number of assumptions and limitations in;

1. specifying the wave characteristics of the local free field ground motion,
2. modelling the dynamic soil properties, especially soil damping on a basis of experimental data and past experiences,
3. idealizing the analytical model of soil-structure system,
4. treating the non-linear soil behavior by the equivalent linear method, which uses strain compatible shear moduli and damping values,
5. coping with possible separation between soil and structure, and
6. computing the response of the model by numerical techniques.

As a consequence, a computed result of structural response may be somewhat different from actual response. For this reason, when a SSI analysis method is applied to design calculation, the method should be assured for its capability of predicting reliable results or otherwise rather conservative results for structural response. Such assessment for the methodology can be made by a comparative examination of measured results with their corresponding predicted results. To do this, some good measured data must be available. Although many excellent data are known, the present description will be restricted to a few but significant example data derived from seismic observations and field shaker tests.

Though the validation of the SSI analysis method can be made by the laboratory tests including the shaking table test and centrifuge test, they will be discussed in the other Session SI.

#### CONCEPTIONAL MODEL FOR SSI ANALYSIS

The soil-structure interaction effect contributes positively to the seismic response of rigid structures or embedded structures, except for the problem of so-called site resonance. It follows that, when a conceptual model is made in this direction, the corresponding equation of motion can be given by the following form in the frequency domain:

$$([K_s] + [K] - \omega^2[M])\{u\} = \{Q\} \quad (1)$$

where  $[K_s]$  = frequency-dependent stiffness matrix of soil,  
 $[K]$  = complex stiffness matrix of structure,  
 $[M]$  = mass matrix of structure,  
 $\{u\}$  = vector of nodal absolute displacements.

$[K]$  and  $[K_s]$  include damping in their imaginary parts.  $\{Q\}$  denotes the external force vector acting on nodes. In the seismic environment,  $\{Q\}$  acts on the nodes on the boundary between the soil and basement and is equal to the force vector required to impose the free field motion on the excavation region. It can be written in the form,

$$([K_s] + [K_g] - \omega^2[M_g])\{u_g\} = \{Q\} \quad (2)$$

where  $[K_g]$  = stiffness matrix of the excavated soil volume in air,  
 $[M_g]$  = mass matrix of the excavated soil volume,  
 $\{u_g\}$  = free field displacement vector in the excavated soil region.

When the free field motion is specified by vertically propagating S and P waves,  $[K_g]$  and  $[M_g]$  are equivalent to those of the one-dimensional soil column in air. It leads to

$$([K_g] - \omega^2[M_g])\{u_g\} = 0 \quad (3)$$

except for the bottom of the excavated soil region, because the bottom surface  $\uparrow$  is subjected to the inertia force  $Q_\uparrow$  and moment  $M_\uparrow$  of the soil column,

$$Q_\uparrow = -\omega^2 \sum_{j=1}^{\uparrow} m_{gj} u_{gj} , \quad M_\uparrow = -\omega^2 \sum_{j=1}^{\uparrow} m_{gj} u_{gj} H_j \quad (4)$$

where  $m_{gj}$  = mass of excavated soil at node  $j$ ,  
 $u_{gj}$  = free field displacement at node  $j$ ,  
 $H_j$  = height of node  $j$  above the bottom of the excavated soil.

Therefore, Eq.(1) becomes

$$([K_s] + [K] - \omega^2[M])\{u\} = [K_s]\{u_g\} + \{P\} \quad (5)$$

where  $\{P\}^T = [0, 0, 0, \dots, Q_\uparrow, M_\uparrow]$

For simplicity, Fig. 2 shows an interaction spring model for embedded structures subjected to a lateral ground shaking, as described by Eq. (5). In this configuration, the rocking stiffness produced by the action of friction along the basement wall is included in the rocking stiffness associated with the bottom.

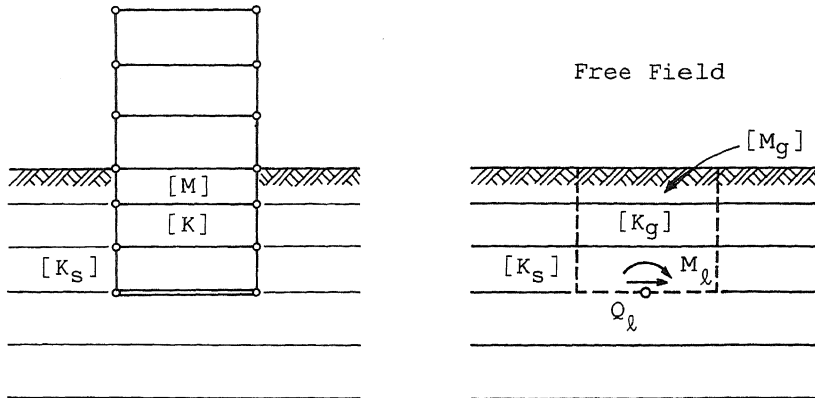


Fig. 1 SSI and free field models in which Eqs. (1), (2) and (3) are applied to

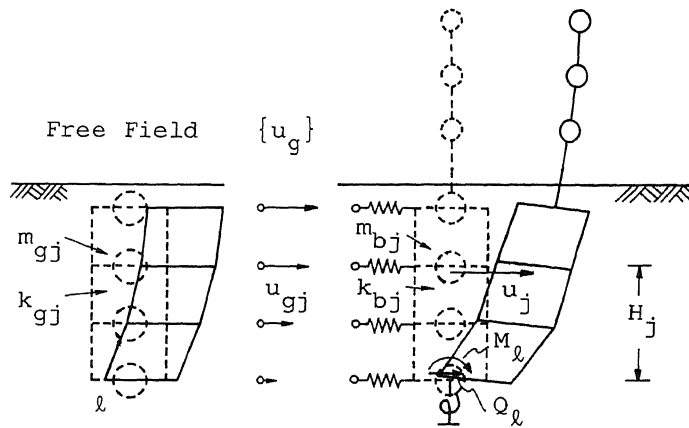


Fig. 2 Interaction spring model subjected to lateral ground shaking

the two steps; the one is a site response analysis for the free field motion and the other is an interaction analysis. So, the seismic observation for the SSI study requires the simultaneous measurements of both structure and free field responses at some critical locations. The measurement of the free field motion aims (1) to obtain the input motion for analysis, (2) to check the shear wave velocities measured by the field seismic survey and to estimate the low-strain damping by using the records during small earthquakes and (3) to determine the equivalent values of shear moduli and hysteretic damping compatible to the strain induced in the soil layers, by using the records during strong earthquakes.

Since the free field response is computed by a one-dimensional analysis of soil column, it is desirable that this condition is acceptable to the soil configuration at the site. This will be realized by a soft soil deposit supported by a stiffer soil with explicit contrast between both moduli. Otherwise, the transfer function between motions at the ground surface and underlying subsurface during small earthquake will become the one shown in Fig. 3 (b) (Ref. 1). Then, it will be difficult to evaluate the equivalent viscous or hysteretic damping compatible to the transfer function (b), while the transfer function (a) is possible to be dealt with.

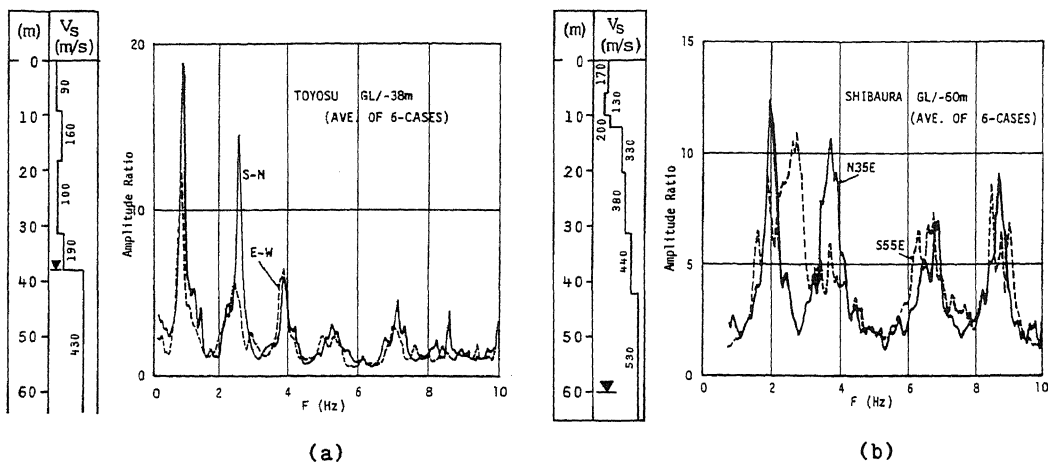


Fig. 3 Examples of transfer function between ground surface motion and underlying subsurface motion, (Ref. 1)

For embedded structures, it is preferable to measure lateral earth pressures and friction forces along the basement walls. As a general trend, it seems that the variation of earth pressures with depth is related to the soil and structural conditions. When the soil is relatively homogeneous and firm and the superstructure is of flexible type, the inertia force of the superstructure may be supported in part by the lateral soil resistance that develops considerably larger in the upper soil layers. On the contrary, when the soil is of soft deposit, the earth pressures due to excitation of the surrounding soil act on the basement walls. These two different states will cause different distributions of story shears in the basement structure, as schematically illustrated in Fig. 4.

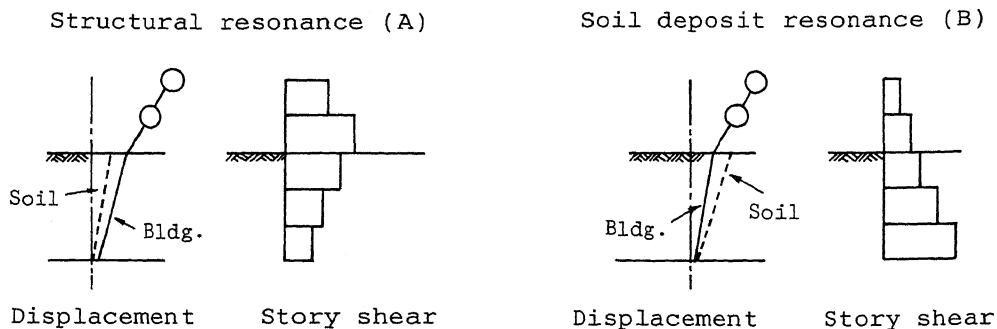


Fig. 4 Story shear distributions for a basement structure produced by structural resonance (A) and soil deposit resonance (B)

#### SEISMIC OBSERVATION

A large number of instruments are located in both actual and model structures to obtain their seismic responses, so that the data will be greatly gathered when future strong earthquake occurs. But, the presently available data are not so much. The examples of actual structures, on which measured data have often been cited as references for validation of the SSI analysis methods, are given in Table 1.

Table 1 Examples of actual structures observed and evaluated from the viewpoint of SSI

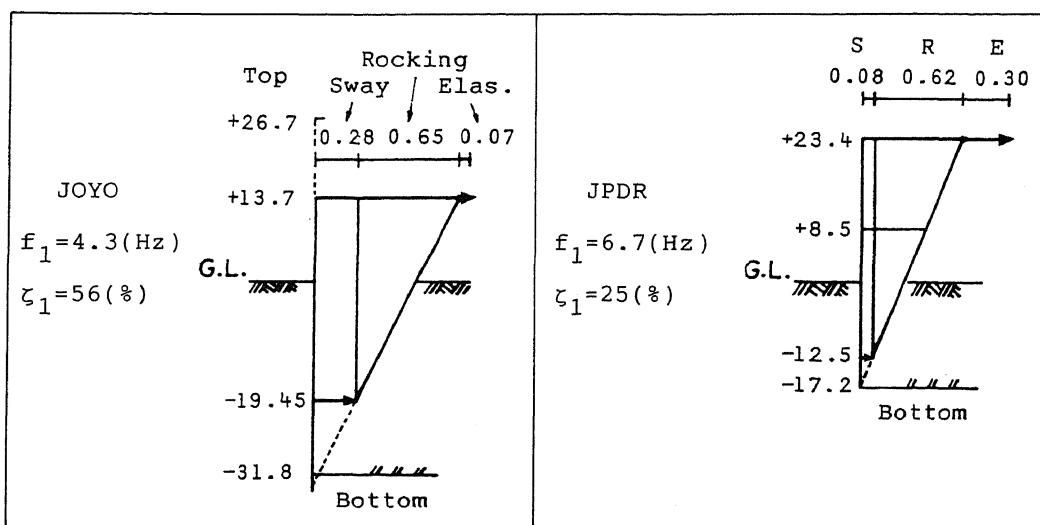
Structure	Main subject of evaluation	Earthquake
Millikan Library building (Ref. 2)	Foundation stiffness	San Fernand Feb. 9, 1971
Humboldt bay power plant (Ref. 3)	Embedment	Ferndale June 7, 1975
Imperial county services bldg.(Ref. 4)	Foundation input motion	Imperial Valley Oct. 15, 1979
Meloland road overpass (Ref. 5)	Bridge-foundation model	Imperial Valley Oct. 15, 1979
JPDR (Refs. 6,7,8)	Embedment	small
JOYO (Refs. 9,10)	Embedment	small
Takenaka experiment building (Refs. 11,12)	Pile foundation	moderate

At the present Session, the latter three cases will be reviewed as good example structures affected greatly by SSI. As for model structures, the two examples will be presented to this Session.

Embedded structures The two embedded structures shown in Figs. 5 and 8 have often been referred to validate the SSI analysis. The larger building is called 'JOYO', a reactor building. The smaller one is called 'JPDR' (Japan Power Demonstration Reactor) and now being decommissioned. The figures include the layout of accelerometers installed in the structure and in the boreholes placed in the free field. The S-wave velocity profiles are also included. Both buildings were subjected to the forced vibration tests and subsequently to a number of small and moderate earthquakes.

The forced vibration test results of the two structures are shown in Table 2 which includes their first mode frequencies, associated damping ratios and mode

Table 2 Forced vibration test results of two embedded structures, (Ref. 6,9)



$f_1$  : 1st mode frequency ,  $\zeta_1$  : 1st mode damping ratio

shapes. From this table one finds that in each case the displacement due to SSI had a considerable portion of the total displacement and it caused a large amount of damping.

The two plots of transfer functions of JPDR are shown in Fig. 6 to exhibit its frequency characteristics from the aspect of SSI. Each is given as an average for several earthquake events. The transfer function  $(S_2)/(G_1)$  denotes the ratio of the spectral amplitude of the structural motion at the operating floor to that of the soil motion at the foundation base depth. Likewise, the transfer function  $(G_2)/(G_1)$  denotes the ratio of the spectral amplitude of the ground surface motion to the soil motion at the foundation base depth. Both transfer functions are found to be close to each other, except for the frequency range greater than 10 Hz. This means the structural response was controlled greatly by the soil response, because the primary modal frequency of the structure related to SSI is 6.7 Hz and is larger than that of the soil deposit that is 4 Hz. Fig. 7 shows an estimate of soil damping value distribution determined by the system identification technique which dealt with the measured transfer function  $(G_2)/(G_1)$  of the free field motions at JPDR. The dotted line in Fig. 6 is the calculated transfer function by using the above soil damping, for comparison. Although the damping values of the lower layers are found to be larger than those expected by the material damping, they show only apparent values which produced a least squares fit between measured and calculated transfer functions in the relatively low frequencies. Therefore it caused a reduction of the calculated transfer function from the measured one in the higher frequency range. This discrepancy is a problem to be resolved in future.

Fig. 8 shows plots of the profile of the maximum acceleration in the free field as well as in the structure of JOYO for different earthquakes. In the figure, the maximum acceleration is normalized by the maximum acceleration at the base rock with a depth of -130 m and shown in the form of amplification factor. The inspection of the figures exhibits the followings:

1. The horizontal response of soil in the free field reveals a marked increase in the upper layer above about 18 m deep, while no significant variation is found in the lower layers. The maximum amplification factors are 2 or 3 at the ground surface.
2. The horizontal response of the structure is slightly amplified at upper floors above the ground level, while it is rather deamplified at the basement floors.

Fig. 9 shows the transfer functions of JOYO, which were calculated as averages of the spectral ratios for selected seven earthquakes. The transfer function  $(F1)/(G4)$  between the foundation motion and the ground surface motion is unity in the low frequency and decreases rapidly with increasing frequency until 4 Hz, beyond which the function is left unchanged. In addition, the function  $(F1)/(G4)$  is found to be close to  $(G2)/(G4)$ , which denotes the transfer function between the foundation level motion and the ground surface motion in the free field, except  $(G2)/(G4)$  has larger amplitude in the frequency range higher than 10 Hz. In the figure, the fine lines indicate the calculated results and are added by the writer for comparison. Such measured result supports the well-known judgement that the foundation response at its base can be approximated by the free field response at a depth close to that of the foundation base.

File-supported building Takenaka experiment building is a two-story reinforced concrete structure and was constructed with special purpose of seismic observation of the full-scale model for a structure supported on pile foundation in a soft soil deposit. The floor plan and section of the building are depicted in Fig. 10, where the layout of instruments are included. The piles are of cast-in-place reinforced concrete with length of 43.3 m and diameter of 1.1 m. The instrumented pile designated by  $P_i$  are equipped with the seven strain gauges to detect the

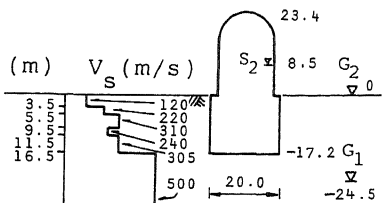


Fig. 5 Outline of JPDR and  $V_s$  distribution, (Ref. 6)

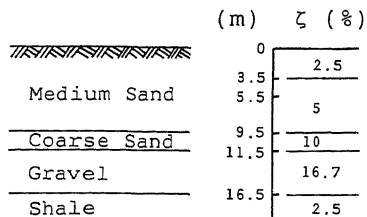


Fig. 7 An estimate of soil damping, JPDR, (Ref. 6)

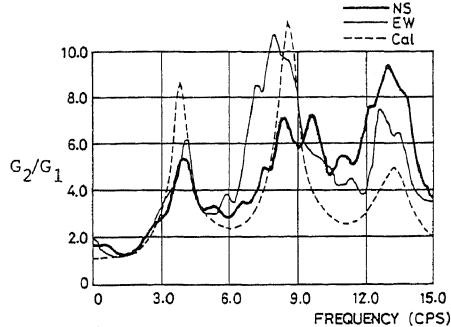
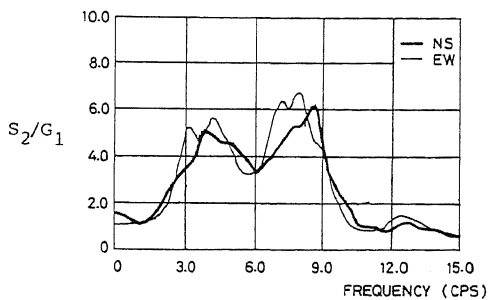


Fig. 6 Two transfer functions of  $(S_2)/(G_1)$  and  $(G_2)/(G_1)$  of JPDR. Measurement locations are shown in Fig. 5, (Ref. 6)

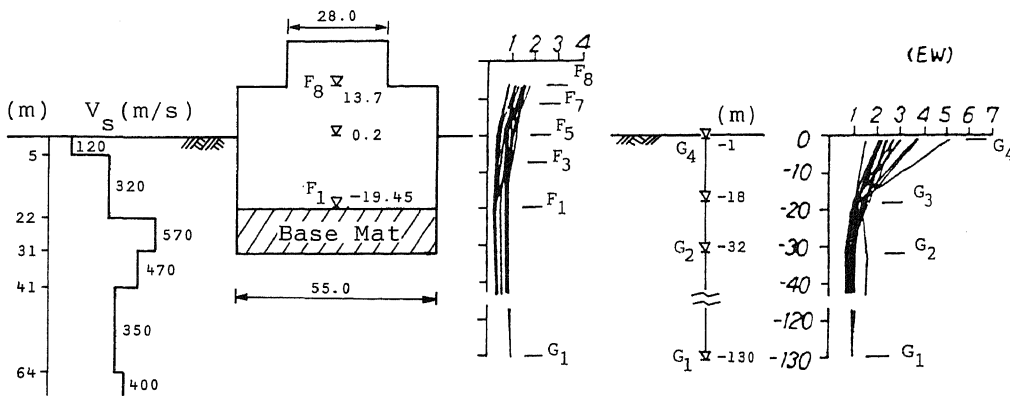


Fig. 8 Outline of JOYO,  $V_s$  distribution and amplification factors of accelerations in structure and soil, (Ref. 10)

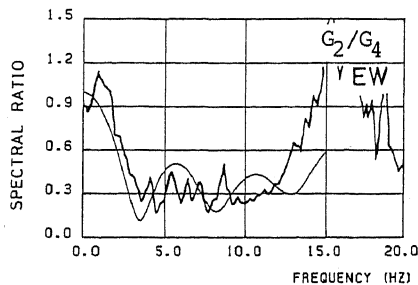
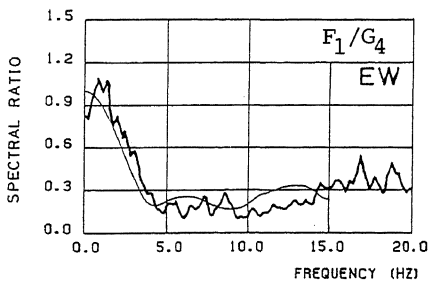


Fig. 9 Two transfer functions of  $(F_1)/(G_4)$  and  $(G_2)/(G_4)$  of JOYO. Measurement locations are shown in Fig. 8, (Ref. 10)

flexural strains of the pile at its different depths. These gauges are designated by S1 to S7 in the figure. Accelerometers are also installed and denoted by F1 and F2. To measure the soil response, the four accelerometers are installed in the neighboring boreholes and designated by G1, G2, G3 and G7. The accelerometers for recording the building response are located at B1 and B2. The soil constants in the analysis were obtained by the seismic logging conducted in the boreholes.

Since the seismic observation initiated in 1982, many records have been obtained. Fig. 11 shows plots of averaged spectral amplitude ratios of B2/G1, B1/G1 and G4/G1. From the figure, one finds the dominant frequency of the soil deposit is about 1 Hz. On the other hand, according to the forced vibration test, the structure has the dominant frequency of 5.5 Hz. It follows that the structural response of interest was also controlled by the soil response, as found by the similarity in both spectra.

Currently used analytical models of pile foundations are (1) Winkler model, (2) the beam model in an elastic or viscoelastic medium, and (3) the finite element model. In this study the simulation analysis was performed by using plane strain finite element model. The input motion to the base of the model was the acceleration time history recorded at a depth of -44 m in the nearby borehole during the earthquake that the maximum acceleration at the ground surface was 90 Gals. Fig. 12 shows the comparison of the calculated and measured results which are plotted for the distribution of the maximum horizontal accelerations and maximum flexural strains with depth. The principal features of the results are as follows:

1. The computed responses were obtained in a somewhat conservative side, compared with the measured responses.
2. The computed flexural strains at intermediate depths were larger than the measured ones and reflected more apparently the change of stiffnesses between layers.

The above remarks, however, are not general, since the piles were controlled considerably by the surrounding soil response, while the pile foundations had been distorted rather by the action of inertia force of superstructures.

The analyses conducted up to data are based on linear methods of soil-pile interaction analysis, because the maximum acceleration at the ground surface is less than 0.1 g. In future, it is expected that seismic observation will be made during strong ground motion, by which one will observe the nonlinear behavior of soil around piles.

#### FIELD TEST

Field tests consist of the shaker test and explosive test. The explosive test is excellent in providing the model structure with a high intensity of shaking and in determining not only the actual impedance functions but also the actual foundation input motion, though the wave characteristics are different from those of real earthquake. One of the SIMQUAKE tests (Ref. 13,14) had a special interest on non-linear rocking response of model containment structure subjected to ground shaking from buried explosion. This test gave good data for non-linear rocking response based on the development of a gap between the structure and the surrounding soil and compaction of soil at the soil-structure interface.

The representative subjects in the linear soil-structure interaction analysis is to obtain the impedance functions for surface and embedded foundations. A number of shaker tests of actual and model mat foundations were carried out and compared with the predicted results. Since the recent analysis methods are



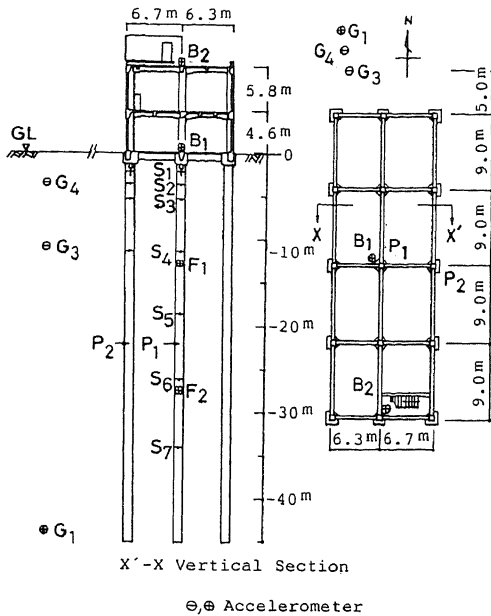


Fig. 10 Vertical section and floor plan of pile-supported structure, including layout of instruments, (Ref. 11)

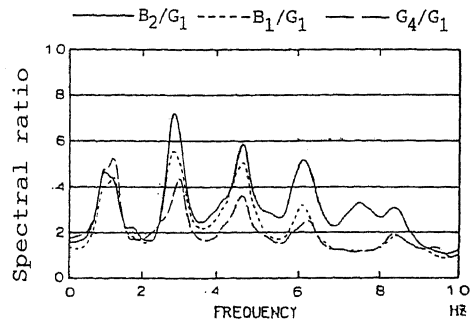


Fig. 11 Averaged Spectral ratios of nearby soil response and structural response, (Ref. 11)

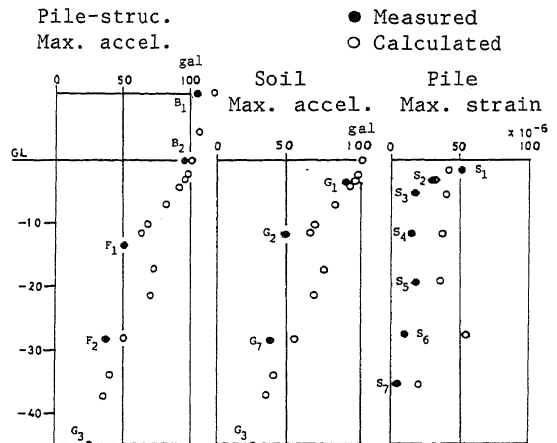


Fig. 12 Comparisons of measurement and calculation for maximum accelerations of soil-pile-structure response and maximum strains of pile, (Ref. 11)

capable of treating a horizontally layered soil model and most test foundations rested on layered soils, the predicted results have been found to be better correlated with the test results. A typical example for these will be reviewed later.

As the shaker test is usually conducted with a low level of excitation, the test results must be sometimes modified to take into account the nonlinear soil effects for its application to design purpose. Alternatively, a heavy shaker test could excite a structure in the same level as actual response probably occurred during strong earthquake motion. This test gave also good data concerning nonlinear rocking response of a full size containment (Ref. 15).

Shaker test of a surface foundation on firm soil. The impedance functions for a surface rigid foundation resting on rocks are hardly affected by the intensity of excitation, because the induced strains of rock are very low. So, it may be said that the measured values of the impedance functions for such foundations are most reliable and useful to application to design analysis of actual foundations. For this purpose, many vibration tests have been carried out for large-scale foundation models on rocks or firm soils (Ref. 16,17). In evaluating these tests and others, it is clear that the experimental impedance functions are in good agreements with the theoretical functions based on the homogeneous half-space theory, if the foundation and soil satisfy the conditions indicated in Table 3 (Ref. 18). Here, the conditions specify the foundations and soils, for which a homogeneous half-space model may be allowed to be applied as a substitute of a one-layer overlying a half-space model.

Table 3 Foundation and soil conditions for application of homogeneous half-space theory (Ref. 18)

Homogeneous half-space model	Foundation and soil conditions
Having the soil properties the same as those of the underlying half-space	$Z_1/\#\bar{A} \leq 0.02$
Having the soil properties the same as those of the top layer	$Z_1/\#\bar{A} \geq 2.0$ $a_0 \geq 1.0$
Having equivalent S-wave velocity. Thus, the half-space produces the static stiffness of surface foundation in agreement with that on original layered soil	$0.02 < Z_1/\#\bar{A} < 2.0$ $0.8 \leq V_{S1}/V_{S2} < 1.0$ $a_0 \geq 1.0$

$Z_1$  = thickness of the top layer,  $A$  = plan area of foundation,  
 $V_{S1}$  = shear wave velocity of the top layer,  $a_0 = \omega\#\bar{A}/V_{S1}$   
 $V_{S2}$  = shear wave velocity of the underlying half-space,

Therefore, the case that dose not satisfy the conditions in Table 3 must be treated by a layered soil model. Fig.13 shows a view of the example foundation (Ref. 19) for this case. The foundation is made of reinforced concrete. The dimensions are 12 m in both length and width and 9.5 m in height. The weight is 3,100 tonf. The soil velocities are also depicted as results of in-situ investigation due to the P-S seismic logging and downhole S-wave velocity measurement. The site primarily consists of three layers of coarse or dense granite. The first layer just beneath the foundation has the shear wave velocity of about 0.5 km/sec with the thickness of about 1 m. This layer was probably disturbed by blast during excavation. The second layer is weathered granite and has the shear wave velocity of about 1.1 km/sec. The third layer is the underlying base rock with the shear wave velocity of 1.8 km/sec.

Table 4 shows the measured natural periods and damping ratios associated with the first modes along the x, y and z axes. The mathematical model was developed in accordance with the analysis method that solves numerically the indirect boundary integral equation involving the 3-dimensional Green's function for the thin-layered elastic soil model. The foundation was a solid cube and the shaker force was applied along the symmetric axis. Nevertheless, the foundation was excited with six degree of freedom during the forced vibration test. This might be caused from inhomogeneity of the rock materials and irregularity of the rock surface, where the rock and foundation were bonded by concrete. It resulted that the measured impedance functions were to be determined in reference to the center

of rigidity of the bottom of the foundation. On the other hand, the calculated impedance functions were referred to the center of gravity of the bottom surface. Both results are compared in Fig. 14 and found to be in good agreement. This means properly that the impedance function with respect to the center of rigidity of the bottom surface gives an averaged stiffness over the contact area which consists of many portions with different stiffnesses.

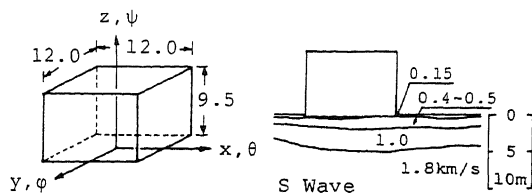


Fig. 13 Outline of test foundation, (Ref. 19)

Table 4 Forced vibration test results, (Ref. 19)

	$f_1$	$\zeta_1$
Horizontal	14.9~15.2	7.9~8.8
Vertical	30.0~32.5	14.7~19.4

$f_1, \zeta_1$  = 1st mode frequency and damping ratio

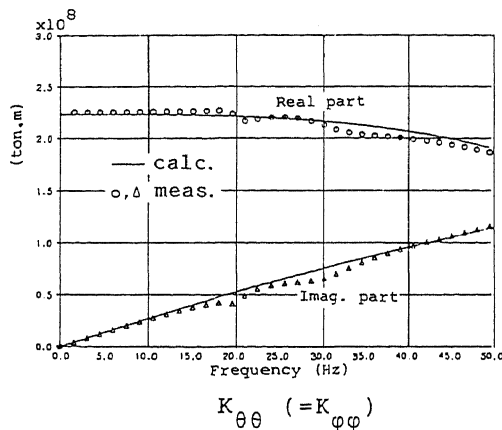
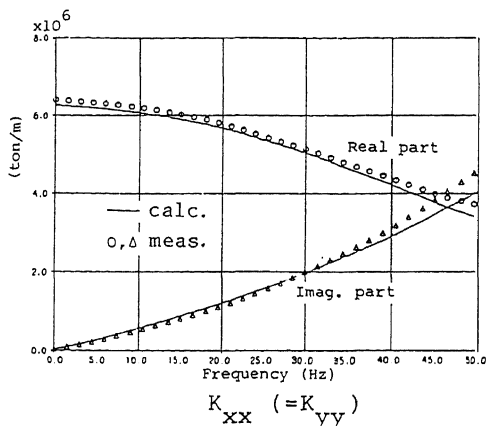


Fig. 14 Comparisons of measured and calculated impedance functions of swaying,  $K_{xx} (=K_{yy})$  and rocking,  $K_{\theta\theta} (=K_{\varphi\varphi})$ , (Ref. 19)

### CONCLUSIONS

1. The most comprehensive data to validate seismic SSI analyses are given by seismic observation of soil and structure responses during a strong nature earthquake. However, such observation data are very little available now, so that it is desirable to instrument a number of structures relevant to SSI in the seismic zones.
2. Most SSI analyses assume the site consisting of horizontal layers laterally extended and supported by a stiffer soil or rock formation. It follows that the actual site is preferable to have a soil configuration close to this ideal one, because of making it possible to identify the soil parameters, especially soil damping from the measured data.
3. The 3-dimensional SSI analysis method capable of treating linearly elastic, horizontally layered half-space soil model can predict well the measured impedance functions for a rigid surface foundation resting on firm soil.

#### REFERENCES

1. H. Yokota, "Earthquake observations and analyses of soft soils in Tokyo," (in Japanese), 5th Symposium on Ground Shaking, Architectural Institute of Japan, pp. 39-44, 1977.
2. J.E. Luco, M.D. Trifunac and H.L. Wong, "On the apparent change in dynamic behavior of a nine-story reinforced concrete building," Bull. Seismo. Soc. Am., Vol. 77, No. 6, pp. 1961-1983, 1987.
3. J.E. Valera, H.B. Seed, C.F. Tsai and J.Lysmer, "Soil-structure interaction effects at the Humbolt day power plant in the Ferndale Earthquake of June 7, 1975," Report No. UCB/EERC-77/02 Earthquake Engineering Research Center, University of California, Berkeley, January 1977.
4. V.W. Lee, M.D. Trifunac and C.C. Feng, "Effects of foundation size on Fourier spectrum amplitudes of earthquake accelerations recorded in buildings," Soil Dynamics and Earthquake Engineering, Vol. 1, No. 2, pp. 52-58, 1982.
5. S.D. Werner, J.L. Beck and M.B. Levine, "Seismic response evaluation of Meloland road overpass using 1979 Imperial Valley earthquake records," Earth. Eng. Struct. Dyn., Vol. 15, pp. 249-274, 1987.
6. T. Iwatate, K. Hanada, et al., "Dynamic properties of JPDR based on earthquake observations and forced vibration tests," Trans. 8th SMiRT, Vol. K(b), pp. 381-386, 1985.
7. T. Takeda et al., "Embedment effect of real nuclear power reactor building and characteristics of different analytical models," Trans. 9th SMiRT, Vol. K2, pp. 1155-1160, 1987.
8. T. Iwatate "Earthquake response analysis of JPDR (Japan power demonstration reactor), Summaries of papers," 19th meeting on earthquake engineering research, Japanese Society of Civil Engineers, pp. 469-472, 1987.
9. T. Ueshima et al., "Earthquake response characteristics of large structure "JOYO" deeply embedded in quaternary ground, (Part 1), Dynamic characteristics of the structure under forced excitation and evaluation of embedment effect," Proc. 7th Japan Earthquake Engineering Symposium, pp. 805-810, 1986.
10. Y. Sawada et al., "Earthquake response characteristics of large structure "JOYO" deeply embedded in Quaternary ground, (Part 2), Earthquake observation results and evaluation of embedment effect," Proc. 7th Japan Earthquake Engineering Symposium, pp. 889-894, 1986.
11. M. Sugimoto et al., "Earthquake observation of structure with pile foundation on soft layer, Part 6 - Simulation analysis of pile foundation by Oct. 4, 1985 earthquake records," Summaries of technical papers, Annual meeting, Architectural Institute of Japan, Structures 1, pp. 539-540, 1986.
12. Y. Abe et al., "Dynamic behavior of pile foundation during earthquakes," Proc. 8th WCEE, Vol. III, pp. 585-592, 1984.
13. C.J. Higgins, "Ground motion induced interface pressures," Proc. ASCE Geotec. Eng. Div., Speciality Conference, Earthquake Engineering and Soil Dynamics, Vol. 1, pp. 492-511, 1978.
14. D.K. Vaughan and J. Isenberg, "Non-linear rocking response of model containment structures," Earthq. Eng. Struct. Dyn. Vol. 11, pp. 275-296, 1983.
15. H. Werkle and G. Waas, "Computed versus measured response of HDR reactor building in large scale shaking tests," Trans, 9th SMiRT, Vol. K2 pp. 479-484, 1987.
16. T. Ueshima et al., "Estimate of dynamic stiffness and by forced excitation test of foundation on bedrock(Part 1)," Trans. 9th SMiRT, Vol K1, pp. 249-254, 1987.
17. K. Hirata et al., "Estimate of dynamic stiffness and by forced excitation test of foundation on bedrock(Part 2)," Trans. 9th SMiRT, Vol. K1, pp. 255-260, 1987.
18. M. Niwa, "Experimental study on soil-foundation interaction on a layered ground," Doctor's Dissertation, Univ. of Tokyo, pp. 247-248, 1985.
19. Y. Yasui et al., "Vibration test of concrete block on a hard rock and simulation analysis," Proc. 7th Japan Earthquake Engineering Symposium, pp. 889-894, 1986.